ORIGINAL PAPER

PREPARATION, CHARACTERIZATION, AND PHOTODYNAMIC TREATMENT OF TOLUIDINE BLUE LOADED PLGA NANOPARTICLES ON *PORPHYROMONAS GINGIVALIS*

Kishore Kumar Avula[1], Sravanthi Gujjula[2], Sudheer Aluru[3], Siva Sai Dandu[1], Sameevulla Mohammed[1], Ravindra Reddy Nagi Reddy[1]

[1]Department of Periodontics and Implantology, CKS Theja Institute of Dental Sciences and Research, India
[2]Department of Prosthodontics and Implantology, CKS Theja Institute of Dental Sciences and Research, India
[3]Division of Animal Biotechnology, Sri Venkateswara University, India

ABSTRACT

Introduction: Periodontitis is a chronic inflammatory disease of periodontal tissues, which can lead to tooth loss and significant sub-gingival tissue deformities anaerobic pathogenic bacteria, where *Porphyromonas gingivalis* play a vital role in the pathogenesis of chronic periodontitis. Antimicrobial photodynamic therapy (aPDT) is proposed as an alternative treatment approach due to bacterial resistance.

Objectives: The objective of this study was to prepare and characterize the photodynamic effect of toluidine blue (TB)-loaded PLGA nanoparticles, in combination with a red light on the periodontal microorganism *P. gingivalis*.

Material and methods: The present study include the following methods: 1) preparations, characterization, and optimization of TB-loaded surface PLGA nanoparticles, and 2) bacterial photodestruction mediated by cationic or anionic TB-loaded nanoparticles *in vitro*.

Results: Particle size and zeta potential of cationic TB-loaded PLGA nanoparticles were 24.0 nm and +44.0 mV, respectively. TB loading and release show in sufficient concentrations in killing *P. gingivalis*. Nano-photodynamic therapy with TB-loaded PLGA nanoparticles inhibited 8 log10 the growth of bacteria at concentrations of 6.25-12.5 μg/ml. The minimal bactericidal concentration of TB for 8 log10 CFU reduction (0.5 McFarland) was 12.5 μg/ml.

Conclusions: Nano-photodynamic therapy with cationic TB-loaded PLGA red light is useful in killing *P. gingivalis* than anionic TB-loaded PLGA. It gives future directions and promising results in clinical trials.

Key words: periodontitis, *Porphyromonas gingivalis*, Nano-photodynamic therapy.

J Stoma 2020; 73, 4: 159-169
DOI: https://doi.org/10.5114/jos.2020.98311

INTRODUCTION

One of the most common human oral diseases is periodontitis, characterized by inflammation of periodontal tissues, such as gingiva and tooth-supporting structures. The sites with periodontal disease contain a unique bacterial composition that differs significantly from that observed in healthy places. Periodontal patho-

JOURNAL OF STOMATOLOGY
CZASOPISMO STOMATOLOGICZNE

Address for correspondence: Prof. Ravindra Reddy Nagi Reddy, Periodontics and Implantology, CKS Theja Institute of Dental Sciences and Research, Tirupathi, India, e-mail: cksperio@gmail.com

Received: 07.05.2020 • Accepted: 19.07.2020 • Published: 30.08.2020

gens, such as *Porphyromonas gingivalis*, are commonly found in infected sites. This Gram-negative anaerobic bacterium plays a significant role in the destruction of the host tissue by the expression of proteases [1].

Conventional phase 1 therapy (i.e., scaling and root planing) can achieve a temporary decrease in the subgingival levels of *P. gingivalis* together with other pathogens. However, it is challenging to remove organisms from the majority of deep periodontal pockets by scaling and root planing (SRP) alone, because of the anatomical complexity of the roots, which may contain bifurcation, trifurcation areas, grooves, and concavities, especially in deep periodontal pockets.

The potential periodontal Gram-negative pathogens, including *Aggregatibacter actinomycetemcomitans* and *Porphyromonas gingivalis*, are capable of evading the host tissue defense mechanisms and invading the surrounding soft tissues, disrupting host epithelial barrier, and invading into deeper periodontal tissues. This creates the fear of reorganization and regrowth of bacteria remaining in pockets or the tissues after SRP [2].

Supplemental chemotherapy, with local drug delivery agents introduced into the periodontal pockets is often recommended to regulate the infection to an extent. It is one of the widely accepted approaches in periodontal treatment (mechano-chemotherapy). However, microbial agents present two significant disadvantages.

In general, the first one is the maintenance of stable therapeutic concentration for a sufficient duration of time eradicating a complex mixture of aerobic Gram-positive and anaerobic Gram-negative bacteria, and the second one is the resistance developed by the target microorganisms to antibiotics [3].

Therefore, there has been a concern among periodontal researchers and clinicians to develop a novel model of approach towards the treatment of periodontal diseases. One such development is a non-invasive photochemical approach for bacterial control, known as photodynamic therapy (PDT), to treat oral diseases as it suppresses the periodontal microorganism and increases the benefits of conventional SRP, leading to a successful periodontal treatment [4].

Antimicrobial photodynamic therapy (aPDT) has been suggested as an alternative to overcome the adverse effects of antibiotics as well as the local and systemic use of antibiotics [2]. PDT is defined as an oxygen-dependent photochemical reaction that occurs upon light-mediated activation of a photosensitizing compound that leads to a generation of cytotoxic reactive oxygen species (ROS), predominantly singlet oxygen that is toxic to the microorganisms. The significant advantages of a PDT are its specific bind to the target bacterial cells, no collateral damage, initiation of activity only when exposed to light, and the lack of development of resistant bacterial species, which is familiar with the indiscriminate use of antibiotics [3].

For safe and efficient administration of PDT, the therapy must reach a target cell in optimum concentrations while being least absorbed by other cells failing, which could cause side effects. However, it suffers from two significant hurdles. Firstly, in an aqueous environment, the hydrophobic molecules of photosensitizer tend to aggregate due to the presence of highly planer molecules that originated as a from the π-conjugation extended system. This disables the photoactive property of the molecule, as it can no longer be monomeric to be an active compound. The next hindrance is the inability of a photosensitizer molecule to reach and bind to the diseased cell when PDT is carried out. Hence, notable efforts have been made to deliver and incorporate a monomeric form of active photosensitizer to target cells under *in vitro* conditions [5].

Most of the carriers are nano-sized in various forms, such as nanorods, nanostructures, and nanoparticles, which have developed with recent advancements in nanotechnology. However, before the advent of nanotechnology, liposomes and micelles were nanostructures of detergents and lipids that were extensively used in photodynamic therapy. Fabrication of nanocarrier molecules delivering PS (photosensitizer) needs to address several questions concerning its binding to the carrier vehicle whether it is covalently attached or if it has to be encapsulated non-covalently, and its bioavailability in the system after its delivery. If it is non-biodegradable, then it could be toxic, and for it to be biodegradable, there are a limited number of polymers and lipids useful in this synthesis. It is being discussed if non-covalent attachment of PS to carrier molecule would facilitate its release and effective assimilation into cells. However, according to EPR (effective permeability and retention) hypothesis, a premature release of PS into serum even before the accumulation of nanoparticles at the diseased site may occur [6].

In the wake of the need, drug polymeric nanoparticles have occupied the front seat as drug carriers during PDT. These have several advantages over conventional molecular drugs by being able to carry more enormous quantities of PS to the diseased site, the pliability according to the target surface, the possibility to use it with a wide range of substances as contrast agents and targeting ligands, and to withstand biodegradation in a living system. PLGA (poly (lactic-co-glycolic acid)) is a polymer of lactic acid and glycolic acid that had been loaded with phthalocyanines, chlorins, porphyrins, and hypericin kinds of photosensitizers, and their efficiency evaluated during PDT [6]. FDA-approved PLA (poly-lactic acid) and PGA (poly-glycolic acid) polyester copolymer is nanoparticle matrix of PLGA. It is biocompatible and can get degraded in the living system by natural pathways [7]. Hence, nanoparticles of PLGA have become useful drug carriers in photosensitizer.

As PS gets capsulated by PLGA, it loses its excited state and thereby loses its phototoxicity. However, nanoparticles show a sustained release of PS when incubated with cells. This helps PS to regain its phototoxicity and hence becomes an active photodynamic agent.

Several studies found that 100% elimination of *P. gingivalis* organisms could be achieved with 25 μg/ml [8]. However, some investigators showed that significant *P. gingivalis* elimination could be accomplished with 1 mg/ml, and also stated that photosensitizer agents are challenging to maintain for a sufficient period of time due to elution of agent gingival crevicular fluid [4].

Many advantages are noted with PLGA, such as controlled and consistent degradation properties, and excellent reproducible mechanical and physical properties, including tensile strength, elastic modulus, and degradation rate. As for toxicity, immunogenicity and favoring of infections are lower for pure synthetic polymers like PLGA; it is used as the most frequent vehicle during treatment strategies.

The biodegradable properties of PLGA are superior when compared with its monomers due to the products of its hydrolysis, lactic acid, and glycolic acid, two endogenous and easily metabolized monomers in minimal systemic toxicity associated with the use of PLGA for drug delivery or biomaterial applications. PLGA has a wide range of degradation rates, governed by the composition of chains, both hydrophobic and hydrophilic balance, and crystallinity. The degradation time is 6-12 weeks for PLGA when used as a carrier for any therapeutic purpose [10]. Stability data showed that pure PLGA particles exhibit the expected behavior for lyophobic colloids. The poloxamines and poloxamers of PLGA were added to the PLGA particles to increase the stability, as they presented more hydrophilic character than in poloxamines.

To overcome this problem, in this research study, we developed a novel photodestruction-mediated TB-loaded PLGA nanoparticles that eliminate *P. gingivalis in vitro*.

OBJECTIVES

The present study was designed with two primary objectives: 1) to prepare, characterize, and determine the concentration of TB-loaded PLGA nanoparticles targeting *P. gingivalis in vitro*, and 2) to recognize the efficacy of photodestruction-mediated TB-loaded PLGA nanoparticles that could suppress or eliminate the *P. gingivalis* colonies.

MATERIAL AND METHODS

PREPARATIONS, CHARACTERIZATION, AND OPTIMIZATION OF TB-LOADED SURFACE PLGA NANOPARTICLES

DEVELOPMENT OF TOLUIDINE BLUE OLEATE SALT

Since toluidine blue (TB) is a very hydrophilic photosensitizer, it was found that pure drug could not be efficiently encapsulated in hydrophobic PLGA nanoparticles. To enhance the loading efficiency, we prepared TB-oleate salt by the reaction of TB with sodium oleate. In an atypical process, 50 mg of TB has dissolved in a 5 ml of dehydrated ethanol and a 100 mg of sodium oleate dissolved in a 100 ml of deionized distilled water by stirring with a magnetic stirrer at room temperature. TB in ethanol was added drop-wise to the aqueous sodium oleate solution and stirred to ensure complete mixing. The mixture was kept at room temperature (27°C) for 8 hours to allow the ethanol to evaporate.

Toluidine blue oleate salt, thus formed, was insoluble in water and precipitated out. The toluidine blue oleate was purified from the remaining sodium oleate by chloroform extraction method. TB oleate salt was then confirmed by measuring visible absorbance, where the fatty acid salt has a characteristic redshift compared to the absorbance of free TB [9].

PREPARATION OF TB-LOADED PEO-PLGA NANOPARTICLES

Preparation of polyethylene oxide (PEO)-modified PLGA nanoparticles was carried out by using a solvent displacement method, in which PLGA was dissolved with pluronic F108 (a triblock copolymer of poly(ethylene oxide/poly(propylene oxide)/poly(ethylene oxide)) in acetone in 75-to-15% weight ratio [9]. For TB-loaded PEO-PLGA nanoparticles, TB oleate was added at 10% (w/w) of the polymer in the organic phase.

The organic phase consisted of PLGA, pluronic F108, and TB oleate, and acetone was added drop-wise to precooled deionized distilled water under moderate stirring condition. The stirring speed, acetone-to-water volume ratio, addition speed, and temperature of the dispersion were optimized to generate particles of approximately 200 nm in diameter. Then, the distribution was left stirring at room temperature overnight until the acetone had evaporated. The aqueous dispersion of TB-loaded PEO-PLGA nanoparticles was centrifuged, washed with deionized distilled water, and lyophilized for approximately 48 hours resulting in flowing-free dry powder.

CHARACTERIZATION OF CONTROL AND TB-LOADED PLGA NANOPARTICLES

Plain PLGA, and cationic and anionic TB-loaded PEO-PLGA nanoparticles were characterized for particle size, surface charge or electric potential, with TB load and a release seen.

Nanoparticle size analysis. Plain PLGA, cationic, and anionic TB-loaded PEO-PLGA nanoparticles were dispersed in deionized distilled water for particle size analysis using the Horiba Scientific SZ-100 nanoparticle analyzer light scattering instrument at 90° scattering angle and 25°C. The rate of the number was adjusted in the range of 50-500 kcps by diluting the samples.

Surface charge analysis. Surface charge or electric potential (zeta potential – ZP) measurements were also performed with the Horiba Scientific SZ-100 zeta potential analyzer instrument. The PLGA and TB-loaded PLGA nanoparticles samples were dispersed in deionized distilled water, and the zeta potential values were measured at the default parameters of dielectric constant, refractive index, and viscosity of water.

Scanning electron microscopy. SEM analysis was performed to confirm the size and determine the nanoparticle shape and surface morphology. Freeze-dried samples of PLGA nanoparticles, with and without the encapsulated TB, were mounted on an aluminum sample mount, and were observed using a JEOL JSM-IT500 In Touch Scope (SV university, TPT) field emission scanning electron microscope, and evaluated for shape and surface morphology by SEM.

DETERMINATION OF TB LOAD IN PEO-PLGA NANOPARTICLES

To determine the TB loading capacity in TB-loaded PLGA nanoparticles, a standard curve of toluidine blue was prepared by dissolving the sodium oleate salt at different concentrations ranging from 10 µg/ml to 250 µg/ml in acetone. The absorbance of the solution was measured at 640 nm with Agilent technologies Cary 8454 UV-Visible spectrophotometer. The TB loading in PEO-PLGA nanoparticles was measured by dissolving a known amount of the nanoparticle sample in acetone. The absorbance of this solution at 640 nm was measured, and the amount of incorporated TB was determined using the standard curve. At 10% (w/w) TB loading, the maximum efficiency was 45-55%.

IN VITRO TB RELEASE STUDIES FROM PEO-PLGA NANOPARTICLES

The release of TB from PLGA nanoparticles was evaluated and compared against two different types of cationic and anionic TB-loaded PLGA nanoparticles. TB-loaded PLGA nanoparticles were modified with pluronic F108 and resulted in a negative surface charge, while the other had a positive surface charge. The toluidine blue oleate release was observed in 1% phosphate buffer saline at 37°C and plotted as a total percentage release over 12-hour time points.

BACTERIAL PHOTODESTRUCTION MEDIATED BY CATIONIC AND ANIONIC TB-LOADED NANOPARTICLES *IN VITRO*

The photodynamic effects of free TB and TB-loaded nanoparticles with positive or negative charge to investigate the *P. gingivalis* microorganisms were obtained from natural human plaque samples. The subgingival plaque samples were inoculated into 2 ml of brucella broth (Himedia), supplemented with 0.4-µl/ml vitamin K_1 (Himedia) and 5-µg/ml hemin (Himedia). They were then diluted and plated onto trypticase soy agar (Himedia) with 10% defibrinated horse blood, 5-µg/ml hemin, and 0.4-µl/ml vitamin K_1. The plates were incubated in an anaerobic atmosphere for 7 to 10 days. The bacteria grown were selected based on size, color, shape, and staining. Fluorescence test by long-wave UV light was performed to distinguish black-pigmented, anaerobic, and Gram-negative rods *P. gingivalis* with other Gram-negative rods. *P. gingivalis* were harvested from plates and re-suspended in brain heart infusion (BHI) broth. A spectrophotometer was used to measure cell numbers (wavelength, 600 nm; 0.1 optical density unit equals to approximately 10^8 cells/ml) in 1-ml cuvettes.

DETERMINATION OF MINIMUM INHIBITORY CONCENTRATION (MIC)

In the present study, the serial tube dilution technique was followed based on the protocols of the Clinical and Laboratory Standards Institute (CLSI) [11]. The stock solution was first prepared by mixing 1 ml of the prepared TB-loaded PLGA nanoparticles (NP) formulation in 10 ml of double-distilled water to achieve a drug concentration of 50 µg/ml. For the preparation of bacterial suspension, brain heart infusion (BHI) broth was used as the culture medium to support the growth of bacteria. Transferring cultured bacteria into the test tubes containing 2 ml of BHI medium attained culture suspension. The *P. gingivalis* strains were adjusted for 0.5 McFarland turbidity standards (10^8 colony forming units [CFU]/ml) to check the MIC of TB-loaded PLGA nanoparticles. In the first tube, 100 µl of stock solution was added into the 300 µl of BHI broth to make a volume of 400 µl, from which nine serial dilutions were prepared in separate test tubes containing 200 µl of BHI broth. To each serially diluted tube, 200 µl of the previously developed *P. gingivalis* bacterial suspension was added and incubated for 48 hours in an Himedia anaerobic jar, with a gas pack at 37°C. A test tube containing only pure *P. gingivalis* (clinically isolated and verified bacterial strain of ATCC 33277 was used as a standard control) bacterial culture was used as a positive control. After completion of the 48 hours incubation period, the optical density values (OD) was measured using a Systonic microprocessor photocolorimeter. MIC was defined as the minimum concentration of the TB-loaded PLGA nanoparticles that caused 20% of inhibition in the growth of the test organism. Independent tests were performed for cationic and anionic nanoparticles. These results formed the basis for further investigations. The percentage of bacterial inhibition by

TB-loaded PLGA nanoparticles was computed using the following equation:

$$\text{percentage of P. gingivalis inhibition} = \frac{OD\ \varepsilon\ control - OD\ in\ test}{OD\ \varepsilon\ control} \times 100$$

NANO-PHOTODYNAMIC TREATMENT FOR BACTERIAL SUSPENSIONS

For the nano-photodynamic treatment of *P. gingivalis* aliquots of bacterial suspensions (10^8/ml) were placed in sterile microcentrifuge tubes and centrifuged (7,000 rpm for 4 minutes). TB-loaded PLGA nanoparticles (both cationic and anionic) or free TB and phosphate-buffered saline (PBS) were added to the supernatants with a concentration of 10 µg/ml to 100 µg/ml. Cultures were tetraplicated and re-suspended with nanoparticles or free TB and placed in the wells of 32-well plates for 5 min before the procedure. All plates were kept covered during the illumination to maintain the purity of the culture. It was followed by irradiation with red laser light for 5 min (100 mW/cm^2, 30 j/cm^2), further to which, the bacterial suspensions underwent serial dilutions in BHI broth; 100 µl aliquots were plated on blood agar plates for anaerobic incubation for seven days. The following experimental groups were used:

1) no laser light/non-TB nanoparticles (control),
2) treated only with laser light,
3) treated only with anionic TB-loaded nanoparticles,
4) treated only with cationic TB-loaded nanoparticles,
5) treated only with free TB,
6) treated with anionic TB-loaded nanoparticles and light,
7) treated with cationic TB-loaded nanoparticles and light,
8) treated with free TB and light.

The primary endpoint for evaluation was the mean number of colony-forming units (CFU) per group [9].

RESULTS

PARTICLE SIZE ANALYSIS

The mean particle size and polydispersion index (PI) of the plain PLGA nanoparticles (Figure 1A), anionic TB-loaded PLGA nanoparticles (Figure 1B), and cationic TB-loaded PLGA nanoparticles (Figure 1C) were determined by dynamic light scattering (DLS) technique, using the Horiba Scientific SZ-100 nanoparticle analyzer. The mean particle size for the prepared plain PLGA nanoparticles, anionic TB-loaded PLGA nanoparticles, and cationic TB-loaded PLGA nanoparticles were 22.2 nm, 23.0 nm, and 24.0 nm, with a PI of 6.983, 15.238, and 21.893, respectively. The prepared TB-loaded PLGA nanoparticles had a narrow distribution range (Table 1).

SURFACE CHARGE/ZP ANALYSIS

ZP measurement of the plain PLGA nanoparticles, anionic TB-loaded PLGA nanoparticles, and cationic TB-loaded PLGA nanoparticles was determined by the DLS technique, using the Horiba Scientific SZ-100 nanoparticle analyzer. The ZP of the prepared plain PLGA nanoparticles (Figure 2A), anionic TB-loaded PLGA N nanoparticles (Figure 2B), and cationic TB-loaded PLGA nanoparticles (Figure 2C) were found to be –14.5 mV, –34.30 mV, and +44.50 mV, respectively (Table 1).

SCANNING ELECTRON MICROSCOPY (SEM)

The prepared nanoparticles were observed for size, shape, morphology, and occurrence of aggregation phenomenon using JEOL JSM-IT500 InTouchScope™ scanning electron microscope. Plain PLGA nanoparticles (Figure 3A), anionic TB-loaded PLGA nanoparticles (Figure 3B), and cationic TB-loaded PLGA nanoparticles (Figure 3C) were well-defined, spherical in shape, smooth-surfaced, and non-porous. The nanoparticles were relatively uniform in size and distribution; however, some agglomeration was observed.

DETERMINATION OF TB LOAD IN PLGA NANOPARTICLES

The amount of incorporated TB was determined using the standard curve. At 10% (w/w) TB loading, the maximum efficiency was 45-55% found by spectrophotometric analysis.

IN VITRO, TB RELEASE STUDIES FROM PEO-PLGA NANOPARTICLES

Drug release was studied using spectrometry under continuous analysis in vitro for 12 hours, taken at regu-

TABLE 1. Nanoparticle size and zeta potential of plain PLGA, TB-loaded anionic, and TB-loaded cationic nanoparticles

Sample name	PLGA nanoparticles	Negative TB-PLGA	Positive TB-PLGA
Mean nanoparticle, diameter (nm)	22.2 ± 2.2	23.0 ± 1.1	24.0 ± 1.6
Mean zeta, potential (MV)	–14.5 ± 0.44	–34.30 ± 0.12	44.5 ± 1.43

A

2019.03.28 12:05:20

HORIBA Scientific

HORIBA SZ-100 for Windows [Z Type] Ver2.00

SZ-100 Measurement Results

201801031304002.nsz

Measurement Results

Date	:	Wednesday, January 03, 2018
Measurement Type	:	Particle Size
Sample Name	:	PLGA PLAIN NANO PARTICLES
Scattering Angle	:	90
Temperature of the Holder	:	25.2 °C
Dispersion Medium Viscosity	:	0.892 mPa·s
Transmission Intensity before Meas.	:	31541
Distribution Form	:	Standard
Distribution Form(Dispersity)	:	Polydisperse
Representation of Result	:	Scattering Light Intensity
Count Rate	:	69 kCPS

Calculation Results

Peak No.	S.P.Area Ratio	Mean	S. D.	Mode
1	1.00	22.2 nm	0.9 nm	23.0 nm
2	---	--- nm	--- nm	--- nm
3	---	--- nm	--- nm	--- nm
Total	1.00	22.2 nm	0.9 nm	23.0 nm

Cumulant Operations

Z-Average	:	0.5nm
PI	:	6.983

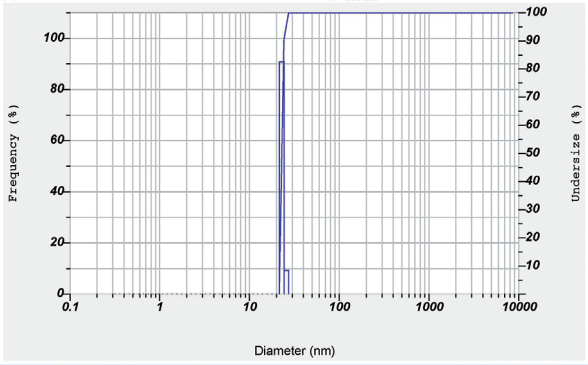

Explore the future HORIBA

1/1

B

2019.03.28 12:05:20

HORIBA Scientific

HORIBA SZ-100 for Windows [Z Type] Ver2.00

SZ-100 Measurement Results

201801031304002.nsz

Measurement Results

Date	:	Wednesday, January 03, 2018
Measurement Type	:	Particle Size
Sample Name	:	ANOINIC PLGA TBO NANO PARTICLES
Scattering Angle	:	90
Temperature of the Holder	:	25.2 °C
Dispersion Medium Viscosity	:	0.892 mPa·s
Transmission Intensity before Meas.	:	31541
Distribution Form	:	Standard
Distribution Form(Dispersity)	:	Polydisperse
Representation of Result	:	Scattering Light Intensity
Count Rate	:	69 kCPS

Calculation Results

Peak No.	S.P.Area Ratio	Mean	S. D.	Mode
1	1.00	23.0 nm	0.9 nm	23.0 nm
2	---	--- nm	--- nm	--- nm
3	---	--- nm	--- nm	--- nm
Total	1.00	23.0 nm	0.9 nm	23.0 nm

Cumulant Operations

Z-Average	:	4.2nm
PI	:	15.238

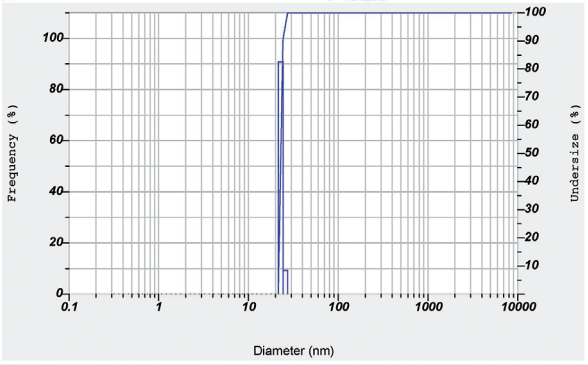

Explore the future HORIBA

1/1

C

2019.03.28 12:05:20

HORIBA Scientific

HORIBA SZ-100 for Windows [Z Type] Ver2.00

SZ-100 Measurement Results

201801031304002.nsz

Measurement Results

Date	:	Wednesday, January 03, 2018
Measurement Type	:	Particle Size
Sample Name	:	CATIONIC PLGA TBO NANO PARTICLES
Scattering Angle	:	90
Temperature of the Holder	:	25.2 °C
Dispersion Medium Viscosity	:	0.892 mPa·s
Transmission Intensity before Meas.	:	31541
Distribution Form	:	Standard
Distribution Form(Dispersity)	:	Polydisperse
Representation of Result	:	Scattering Light Intensity
Count Rate	:	69 kCPS

Calculation Results

Peak No.	S.P.Area Ratio	Mean	S. D.	Mode
1	1.00	24.0 nm	0.9 nm	23.0 nm
2	---	--- nm	--- nm	--- nm
3	---	--- nm	--- nm	--- nm
Total	1.00	24.0 nm	0.9 nm	23.0 nm

Cumulant Operations

Z-Average	:	5.3nm
PI	:	21.893

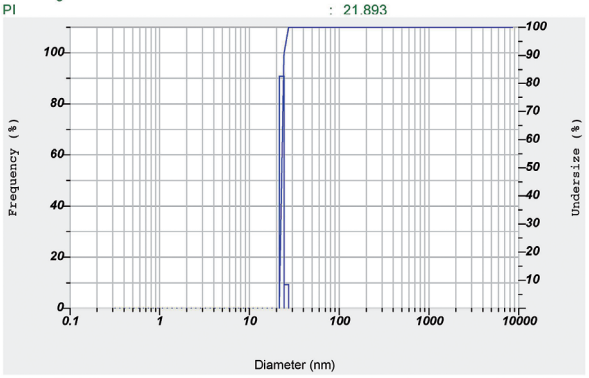

Explore the future HORIBA

1/1

FIGURE 1. A) Mean particle size of plain PLGA nanoparticles. **B)** Mean particle size of anionic TB-loaded PLGA nanoparticles. **C)** Mean particle size of cationic TB-loaded PLGA nanoparticles

A

2019.03.28 12:07:12

HORIBA Scientific

HORIBA SZ-100 for Windows [Z Type] Ver2.00

SZ-100

Measurement Results

201801031312004.nzt

Measurement Results

Date	:	Wednesday, January 03, 2018 1:12:11 PM
Measurement Type	:	Zeta Potential
Sample Name	:	PLGA PLAIN NANO PARTICLES
Temperature of the Holder	:	25.1 °C
Dispersion Medium Viscosity	:	0.893 mPa·s
Conductivity	:	0.121 mS/cm
Electrode Voltage	:	3.3 V

Calculation Results

Peak No.	Zeta Potential	Electrophoretic Mobility
1	-14.5 mV	-0.000004 cm2/Vs
2	--- mV	--- cm2/Vs
3	--- mV	--- cm2/Vs

Zeta Potential (Mean)	:	-0.5 mV
Electrophoretic Mobility Mean	:	-0.000004 cm2/Vs

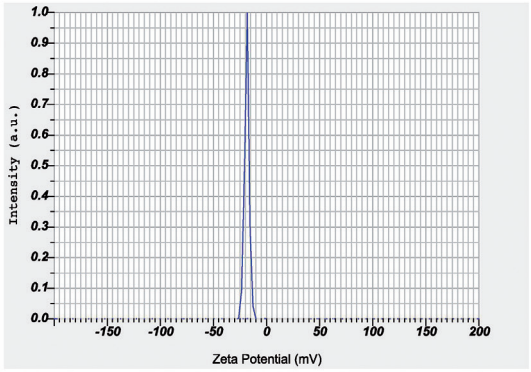

Explore the future HORIBA

1 / 1

B

2019.03.28 12:07:12

HORIBA Scientific

HORIBA SZ-100 for Windows [Z Type] Ver2.00

SZ-100

Measurement Results

201801031312004.nzt

Measurement Results

Date	:	Wednesday, January 03, 2018 1:12:11 PM
Measurement Type	:	Zeta Potential
Sample Name	:	ANOINIC PLGA TBO NANO PARTICLES
Temperature of the Holder	:	25.1 °C
Dispersion Medium Viscosity	:	0.893 mPa·s
Conductivity	:	0.121 mS/cm
Electrode Voltage	:	3.3 V

Calculation Results

Peak No.	Zeta Potential	Electrophoretic Mobility
1	-34.30 mV	-0.000004 cm2/Vs
2	--- mV	--- cm2/Vs
3	--- mV	--- cm2/Vs

Zeta Potential (Mean)	:	-0.5 mV
Electrophoretic Mobility Mean	:	-0.000004 cm2/Vs

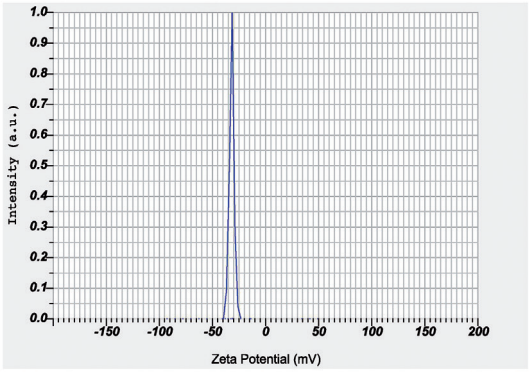

Explore the future HORIBA

1 / 1

C

2019.03.28 12:07:12

HORIBA Scientific

HORIBA SZ-100 for Windows [Z Type] Ver2.00

SZ-100

Measurement Results

201801031312004.nzt

Measurement Results

Date	:	Wednesday, January 03, 2018 1:12:11 PM
Measurement Type	:	Zeta Potential
Sample Name	:	CATIONIC PLGA TBO NANO PARTICLES
Temperature of the Holder	:	25.1 °C
Dispersion Medium Viscosity	:	0.893 mPa·s
Conductivity	:	0.121 mS/cm
Electrode Voltage	:	3.3 V

Calculation Results

Peak No.	Zeta Potential	Electrophoretic Mobility
1	44.50 mV	0.000004 cm2/Vs
2	--- mV	--- cm2/Vs
3	--- mV	--- cm2/Vs

Zeta Potential (Mean)	:	-0.5 mV
Electrophoretic Mobility Mean	:	-0.000004 cm2/Vs

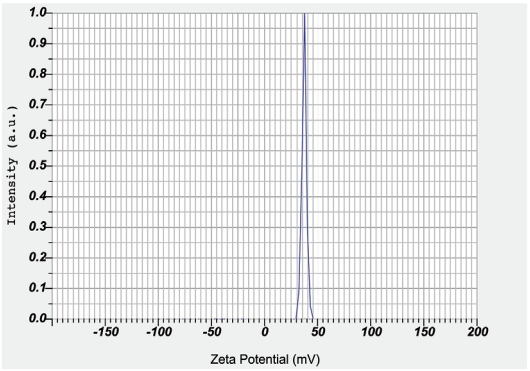

Explore the future HORIBA

1 / 1

FIGURE 2. A) Zeta potential of plain PLGA nanoparticles. **B)** Zeta potential of anionic TB-loaded PLGA nanoparticles. **C)** Zeta potential of cationic TB-loaded PLGA nanoparticles

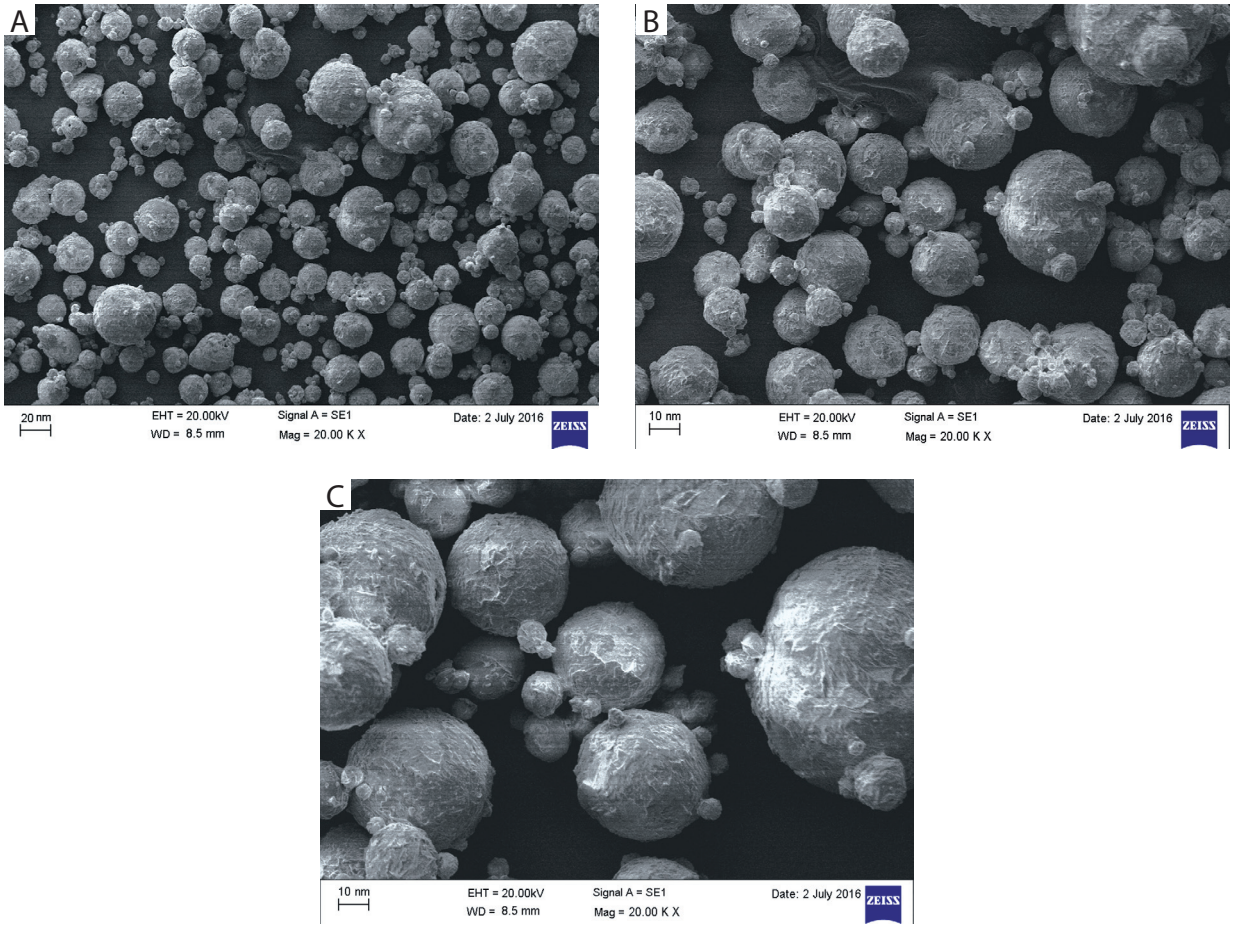

FIGURE 3. A) SEM of plain PLGA nanoparticles. **B)** SEM of anionic TB-loaded PLGA nanoparticles. **C)** SEM of cationic TB-loaded PLGA nanoparticles

TABLE 2. *In vitro* cationic TB release profile of +TB PLGA nanoparticles

S. No	Time (hours)	Cumulative percentage release of anionic TBO from +TBO-loaded PLGA nanoparticles
1.	0	0
2.	1	2.03
3.	2	4.43
4.	3	8.03
5.	4	10.43
6.	5	12.66
7.	6	18.12
8.	7	24.32
9.	8	32.02
10.	9	38.63
11.	10	42.82
12.	11	48.93
13.	12	50.12

TABLE 3. *In vitro* anionic TB release profile of TB PLGA nanoparticles

S. No	Time (hours)	Cumulative percentage release of anionic TB from TB-loaded PLGA nanoparticles
1.	0	0
2.	1	8.33
3.	2	16.43
4.	3	24.66
5.	4	32.12
6.	5	40.32
7.	6	48.02
8.	7	56.63
9.	8	64.82
10.	9	72.93
11.	10	80.12
12.	11	88.16
13.	12	96.33

lar intervals using 1% PBS. Drug release was calculated based on initial concentration to the release at a given point of time. Cationic nanoparticles (Table 2) were released at a slower rate with a total of 30% release, as against 80% total release rate of anionic nanoparticles (Table 3) for 12 hours observations at 37°C temperature (Figure 4).

DETERMINATION OF MINIMUM INHIBITORY CONCENTRATION

Results from minimum inhibitory concentration (MIC) showed cationic nanoparticles to be more effective over anionic nanoparticles. MIC, which was defined to be as the minimum concentration of the TB-loaded PLGA nanoparticles that caused 20% inhibition in the growth of the test organism, was found persistent with cationic nanoparticles, unlike in anionic. The measured OD (mean ± SD) at the concentration of 1.56 µg/ml was 0.498 ± 0.020, which showed 32.23% inhibition of bacterial growth. Hence, MIC of test bacterial strains was recorded as 1.56 µg/ml (Table 4). As cationic nanoparticles showed better results over anionic, in all further investigations, only cationic nanoparticles were utilized.

PHOTODYNAMIC TREATMENT MEDIATED BY CATIONIC AND ANIONIC TBO-LOADED NANOPARTICLES *IN VITRO*

The photodynamic treatment shows the mean percentage of colony-forming units in Table 5. Cationic TB-loaded PLGA nanoparticles (1.56 µg/ml equivalent to TB) and free TB (1.56 µg/ml) led to 98% and 43% killing, respectively (Table 5) (p-value < 0.05 vs. no laser light in no TB [control]).

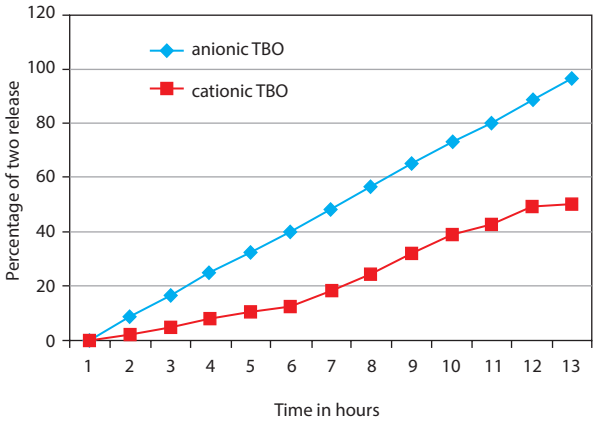

FIGURE 4. Cationic nanoparticles realeased TB much slower than anionic TB nanoparticles. After 12 hours, over 80% of encapsulated TBO was released in PBS at room temperature from anionic nanoparticles and approximately 30% from cationic TB PLGA nanoparticles

TABLE 4. Minimum inhibitory concentration of cationic TB-loaded PLGA nanoparticles

Concentration of serial dilutions (µg/ml)	OD mean ± SD	% inhibition
0.19	0.584 ± 0.017	08.37
0.39	0.552 ± 0.019	16.72
0.78	0.530 ± 0.015	19.56
1.56	0.498 ± 0.020	32.23
3.12	0.487 ± 0.018	44.43
6.25	0.483 ± 0.011	64.91
12.5	0.410 ± 0.025	79.96
25.0	0.150 ± 0.022	88.37
50.0	0.054 ± 0.023	96.12
100.0	0.024 ± 0.020	99.93
Control without cationic TB PLGA nanoparticles	0.598 ± 0.023	

DISCUSSION

Cationic nanoparticles showed promising results over anionic nanoparticles. An infectious microbial disease that results in inflammation of gums, supporting structures of teeth, which ultimately result in loss of attachment and bone resorption are the characteristics of chronic periodontitis. Its etiological factors include the accumulation of plaque at tooth surfaces, gums, and dento-gingival juncture [1].

Complete removal of endotoxins, biofilms, and calculus from the surface of tooth reinstitutes gingival health, which forms the principle of non-surgical periodontal treatment through SRP, including scaling and root planing. However, SRP meticulously removes supragingival and subgingival plaque, calculus, and necrotic cementum, it is not effective in the total eradication of deep-seated microbes, which are situated deep into the periodontal tissues, dentinal tubules, and other inaccessible areas, owing to anatomical complications.

Technological advancements have always been consistent in finding new approaches towards the treatment of periodontal illnesses, as it has been a long-time interest of clinicians and periodontal specialists. Photodynamic treatment is one such non-invasive exploration for including microbial contamination and oral diseases [5], which received considerable applause among the periodontists.

We must consider several challenges while optimization and formulation of a TB-loaded PLGA nanocarrier system. In the first instance, we should formulate the nanocarrier systems to efficiently encapsulate TB at 10% (w/w), to have the desired physical prop-

TABLE 5. Incubation of *Porphyromonas gingivalis* bacteria with TB-loaded nanoparticles (1.56 µg/ml equivalent to TB) for 5 min, followed by exposure to laser red light for 5 min (100 mw/cm^2, 30 j/cm^2) led to > 1 log bacterial killing

	1	2	3	4	5	6	7	8
PG-1	400	320	220	140	234	82	5	120
PG-2	395	295	210	125	226	75	6	112
PG-3	420	300	190	110	213	55	4	102
PG-4	389	280	185	130	245	77	5	132
MEAN	401	298	201	126	229	72	5	116
Bact- viable	100%	74.3%	50.1%	31.4%	57.1%	17.9%	1.2%	28.9%
Bact- killed		25.7%	49.9%	68.6%	42.9%	68.1%	98.8%	71.1%

erties of size (~25 nm in diameter), surface charge, and stability.

Our study shows that PLGA nanocarriers can efficiently encapsulate > 65% TB for cationic and approximately 40% for anionic nanoparticles. The surface morphology was smooth and round for both types of nanoparticles formulations to achieve the desired particle size and move through minute water channels present in biofilms. However, the cationic nanoparticles were able to release the drug at slow-paced for extended periods, unlike those of anionic nanoparticles.

We have optimized the PLGA nanoparticle size, surface charge, and the efficient encapsulation of TB formulation at each step to achieve the desired pharmacological benefit of PDT.

As mentioned earlier, PS loses its phototoxicity when it gets encapsulated in PLGA and on incubation with cells, showing sustained timely release, gaining back its phototoxic property, which forms an activated PDT nano agent [10] with a wide range of beneficial properties, including sustained timely release and non-toxicity in extracellular spaces. On the other hand, TB is a well-known PS to be used in PDT against a spectrum of Gram-positive and harmful oral microbes [12].

Our findings about cationic nanoparticles are supported by literature, which show positively charged PS to be more effectively taken up by PLGA. It has greater phototoxicity against microbes [13], and hence cationic PLGA nanoparticles are likely to serve as better alternatives to neutrally charged nanoparticles. Of late, biodegradable cationic chitosan-made PLGA nanoparticles have been explored in vitro for their gene carrying capacity in the nasal mucosa of mice [14]. The results were promising, where PLGA nanoparticles assisted the delivery of gene, followed by its gene expression with greater efficiency without causing any inflammation.

However, as periodontists, NPDT clinical safety is vital, and we should consider the side effects and risks involved in PDT, which include photosensitizer and photochemical reaction as well as other being the impact of light energy.

The side effects, such as bactericidal activity exhibited by an independent or unbound PS, can be toxic to periodontal tissues. Besides, most PDT dyes attached tightly to periodontal soft tissues, lead to dye retention in periodontal pockets, which could affect the periodontal tissues with attachment and healing.

However, it should be noted that clinical removal of a dye after ever PDT is not feasible, and its retention leads to short-term pigmentation of gums. This would impact the aesthetics of a patient. Hence, in the present study, we made PS to lose its phototoxicity by encapsulating it in PLGA and later, on incubation with cells showing sustained timely release of PS, gaining back its phototoxic property, and formed an activated PDT nano agent.

Red light is an adequate light source being used in PDT. However, precautions need to be taken to protect the eyes of the patient and healthcare staff involved in laser surgery [15]. Additionally, when high-level or diode lasers are continuously used, they lead to thermogenesis, which should be avoided to prevent deeper tissues injuries, such as pulp or alveolar bone [16].

The TB-loaded PLGA photosensitizer gets activated at a wavelength of 620 nm to 720 nm of laser light, which is in the red zone of the light spectrum. In the present study, laser light with a wavelength of 630 nm was used at 0.5 mW laser red light for 5 min (100 mw/cm^2, 30 j/cm^2) of energy. The depth of the laser light penetration was ranging from 0.5 mm to 1.5 mm.

The present study speaks of light-activated TB-loaded PLGA nanoparticles as an antibacterial treatment against *P. gingivalis*. Our *in vitro* study showed cationic TB-loaded PLGA nanoparticles to be more effective over anionic nanoparticles and free TB, when tested against *P. gingivalis*. This could be because of the catatonically charged toluidine blue had bonded to Gram-negative bacterial outer cell membrane, penetrating it, followed by interaction with lipopolysaccharides exhibiting photo-bacterial effect. Hence, we used cationic TB-loaded PLGA nanoparticles to treat chronic periodontitis through PDT.

CONCLUSIONS

The present *in vitro* study has optimized formulations of cationic TB-loaded PLGA nanoparticles that can be used as an addition to standard periodontal therapy to eliminate the periodontal bacteria, especially *P. gingivalis* present in dental plaque.

ACKNOWLEDGMENT

The present research study is a part of Ph.D. Thesis work to Dr. N.T.R University of Health Sciences and Research.

CONFLICT OF INTEREST

The authors declare no potential conflicts of interest with respect to the research, authorship, and/or publication of this article.

References

1. Newman MG, Takei HH, Klokkevold PR, Carranza FA. Clinical Periodontology. 10th ed; 222-223.
2. Braham P, Herron C, Street C, Darveau R. Antimicrobial photodynamic therapy may promote periodontal healing through multiple mechanisms. J Periodontol 2009; 80: 1790-1798.
3. Takasaki AA, Aoki A, Mizutani K, et al. Application of antimicrobial photodynamic therapy in periodontal and peri-implant disease. Periodontol 2000 2009; 51: 109-140.
4. Kömerik N, Nakanishi H, MacRobert AJ, et al. In vivo killing of porphyromonas gingivalis by toluidine blue-mediated photosensitization in an animal model. Antimicrob Agents Chemother 2003; 47: 932-940.
5. Berakdar M, Callaway A, Fakhr Eddin M, Ross A, Willershausen B. Comparison between scaling-root-planing (SRP) and SRP/photodynamic therapy: a six-month study. Head Face Med 2012; 8: 12.
6. Huang YY, Sharma SK, Dai T, et al. Can nanotechnology potentiate photodynamic therapy? Nanotechnol Rev 2012; 1: 111-146.
7. Panyam J, Zhou WZ, Prabha S, Sahoo SK, Labhasetwar V. Rapid endo-lysosomal escape of poly(DL-lactide-co-glycolide) nanoparticles: implications for drug and gene delivery. FASEB J 2002; 16: 1217-1226.
8. Bhatti M, MacRobert A, Meghji S, Henderson B, Wilson M. A study of the uptake of toluidine blue O by Porphyromonas gingivalis and the mechanism of lethal photosensitization. Photochem Photobiol 1998; 68: 370-376.
9. Klepac-Ceraj V, Patel N, Song X, et al. Photodynamic effects of methylene blue-loaded Polymeric nanoparticles on dental plaque bacteria. Lasers Surg Med 2011; 43: 600-606.
10. McCarthy JR, Perez JM, Brückner C, Weissleder R. Polymeric nanoparticle preparation that eradicates tumors. Nano Lett 2005; 5: 2552-2556.
11. CLSI. Methods for Antimicrobial Susceptibility Testing of Anaerobic Bacteria. 9th ed. CLSI standard M11. Wayne, PA: Clinical and Laboratory Standards Institute; 2018.
12. Harris F, Chatfield LK, Phoenix DA. Phenothiazinium based photosensitizers-photodynamic agents with a multiplicity of cellular targets and clinical applications. Curr Drug Targets 2005; 6: 615.
13. Soukos NS, Socransky SS, Mulholland SE, Lee S, Doukas AG. Photomechanical drug delivery into bacterial biofilms. Pharm Res 2000; 17: 405-409.
14. Kumar PS, Griffen AL, Moeschberger ML, Leys EJ. Identification of candidate periodontal pathogens and beneficial species by quantitative 16S clonal analysis. J Clin Microbiol 2005; 43: 3944-3955.
15. Research, Science and Therapy Committee of the American Academy of Periodontology. Lasers in periodontics. J Periodontol 2002; 73: 1231-1239.
16. Takasaki AA, Aoki A, Mizutani K, et al. Application of antimicrobial photodynamic therapy in periodontal and peri-implant diseases. Periodontol 2000 2009; 51: 109-114.